

Orthogonal Transform Multiplexing with Memoryless Nonlinearity: a Possible Alternative to Traditional Coded-Modulation Schemes

Sergey V. Zhidkov, *Member, IEEE*

Abstract—In this paper, we propose a novel joint coding-modulation technique based on serial concatenation of orthogonal linear transform, such as discrete Fourier transform (DFT) or Walsh-Hadamard transform (WHT), with memoryless nonlinearity. We demonstrate that such a simple signal construction may exhibit properties of a random code ensemble, as a result approaching channel capacity. Our computer simulations confirm that if the decoder relies on a modified approximate message passing algorithm, the proposed modulation technique exhibits performance on par with state-of-the-art coded modulation schemes that use capacity-approaching component codes. The proposed modulation scheme could be used directly or as a precoder for a conventional orthogonal frequency division multiplexing (OFDM) transmitter, resulting in a system possessing all benefits of OFDM along with reduced peak-to-average power ratio (PAPR).

Index Terms—Channel capacity, random-like codes, coded modulation schemes, Walsh-Hadamard transform, OFDM, nonlinearity, peak-to-average power ratio

I. INTRODUCTION

A traditional approach for transmitting digital information over a communication link with high spectral efficiency ($\eta \geq 2$ bit/s/Hz) is to combine good error-correcting code with high-order modulation. Over last two decades, several capacity-approaching coded modulation techniques have been proposed, including low-density parity check (LDPC) coded modulation [1, 2], turbo-coded modulation and turbo trellis-coded modulation [3]. In this paper, we propose an alternative bandwidth-efficient modulation technique, which does not rely on any error correction coding in the traditional sense, while still achieving error rates close to the best known coded modulation schemes. Our method is based on serial concatenation of an orthogonal linear transform, such as DFT or WHT, with memoryless nonlinearity. We demonstrate that such a simple signal construction may exhibit properties of random code ensemble, as a result approaching channel capacity if decoded using a maximum-likelihood (ML) decoder.

When the proposed modulation scheme relies on DFT transform, it can be viewed as an OFDM signal distorted by very strong memoryless nonlinearity. In the context of OFDM, any nonlinearity is usually considered a highly undesirable phenomenon. In fact, the sensitivity of OFDM technology to nonlinear distortions is usually cited as a major drawback of OFDM. Nonetheless, in [4], the authors theoretically proved that the bit error rate (BER) performance of

OFDM transmission subjected to strong memoryless nonlinearity can outperform linear transmission, provided that an optimal ML-receiver is used. Moreover, in [5], we proposed a practical message-passing receiver for nonlinearly distorted OFDM signals, showing that the BER performance of hard-clipped OFDM signals can be up to 2 dB better than linear OFDM transmission. In this paper, we go one step further to demonstrate that if the uncoded OFDM signal is distorted by memoryless nonlinearity with certain properties, the resultant signal waveform may achieve BER performance close to the best known capacity-approaching coded modulation techniques. The same performance can also be achieved by replacing DFT in the transmitter with WHT, resulting in simpler hardware/software implementation of the encoder and the decoder.

II. PROPOSED MODULATION TECHNIQUE

A. Achieving capacity by serial concatenation of orthogonal transform and memoryless nonlinearity

Consider the modulation scheme illustrated in Figure 1. In the transmitter, N uncoded real or complex baseband modulation symbols $\mathbf{x} = \{x_k\}$ (e.g. M -QAM, or M -PAM) are first transformed by means of orthogonal block transform and then passed through memoryless nonlinearity block. The signal at the modulator output can be expressed as:

$$s_n = f(z_n), \quad n = 0, 1, \dots, N-1 \quad (1)$$

where $f(z)$ is a memoryless nonlinear function, and

$$\mathbf{z} = \mathbf{F}\mathbf{x}, \quad (2)$$

where $\mathbf{z} = \{z_n\}$, and \mathbf{F} is a $N \times N$ (unitary) orthogonal transform matrix. In this paper, we consider two types of transforms: Walsh-Hadamard transform, and discrete Fourier transform (real-valued or complex).

Let us now assume that the memoryless nonlinear function $f(z)$ can be represented as $f(z) = \underbrace{g(\dots g(g(z)))}_{l\text{-times}}$, where $g(z)$

is a deterministic chaotic map. Thus, $f(z)$ has certain properties of chaotic iterated functions, namely, *sensitive dependence on initial conditions* [6]. Under such assumptions, and if $N \rightarrow \infty$ and $l \rightarrow \infty$, the ensemble of waveforms generated by (1) possesses all major properties of a random code ensemble, because even small modifications in the message sequence $\{x_k\}$ (e.g., in a single bit) lead to:

S. V. Zhidkov is with Cifrasoft Ltd., Izhevsk, Russia, e-mail: sergey.zhidkov@cifrasoft.com.

- a) small modifications, at least, for all samples of the intermediate signal z_n due to the spreading properties of the orthogonal transform operation, and
- b) large (and pseudo-random) modifications for all samples of waveform s_n due to the properties of the nonlinear function $f(z)$.

Therefore, we conjecture that where $f(z)$ has the above-mentioned properties if the waveforms generated by (1) are demodulated using a ML decoder, system performance may approach channel capacity. Unfortunately, brute-force, maximum-likelihood decoding of (1) is prohibitively complex, generally of the order $O(M^N)$, where M is the modulation order. However, as in many practical applications, we can rely on belief-propagation techniques to approximate ML-decoding. A perfect candidate for decoding the signals generated by (1) is the generalized approximate message passing (GAMP) algorithm [7]. Having already been applied to the decoding of clipped OFDM signals in [5], it has demonstrated good performance and reasonably good convergence behavior.

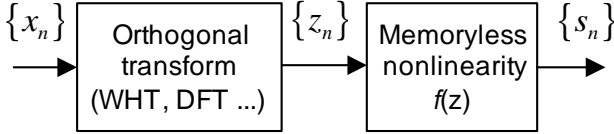


Fig. 1. Proposed modulation scheme

B. GAMP algorithm and its modifications

In the additive white Gaussian noise (AWGN) channel, the model of the received signal can be expressed as

$$y_n = f(z_n) + w_n, \quad n = 0, 1, \dots, N-1 \quad (3)$$

where w_n is the AWGN term with zero mean and variance μ^w . Model (3) is equivalent to a general problem formulation for the GAMP algorithm [7], which belongs to a class of Gaussian approximations of loopy belief propagation for dense graphs. In our decoder implementation, we use the sum-product variant of the GAMP algorithm, which approximates minimum mean-squared error estimates of \mathbf{x} and \mathbf{z} .

During simulation study, we discovered that the convergence behavior and bit and frame error rate (FER) performance of the conventional GAMP algorithm applied to the decoding of (3) may be improved by several simple algorithm modifications. In particular, we used damped version of the GAMP algorithm, which is known to improve convergence for certain mixing matrices [8], and introduced scaling factor for AWGN term variance $\mu^w \rightarrow \alpha\mu^w$. In addition, we implemented the final decision selection and post-processing scheme as will be explained in the next section that helped us overcome certain deficiencies of a conventional GAMP algorithm. To reduce computational complexity we opted to use a version of GAMP algorithm with scalar step-sizes [7]. Note that the scalar step-size version of the GAMP algorithm is optimal for WHT and complex DFT since in both cases $|F_{n,k}|^2 = 1$. Moreover, our experimental study revealed that the performance loss for real DFT case ($|F_{n,k}|^2 \neq 1$) was also marginal.

The GAMP algorithm adapted to our problem is summarized below. The algorithm generates a sequence of estimates $\hat{\mathbf{x}}(t)$, $\hat{\mathbf{z}}(t)$, for $t = 1, 2, \dots$ through the following recursions:

Parameters:

t_{max} the maximum number of iterations,

α the noise scaling factor,

β the damping factor.

Step 1) Initialization:

$$t = 1, \hat{\mathbf{x}}(1) = \mathbf{0}, \tilde{\mathbf{x}}(1) = \mathbf{0}, \boldsymbol{\mu}^x(1) = \mathbf{1}, \hat{\mathbf{s}}(0) = \mathbf{0}$$

Step 2) Estimation of output nodes:

$$\mu_n^p(t) = \frac{1}{N} \sum_{k=0}^{N-1} \mu_k^x(t), \forall n \quad (4)$$

$$\hat{p}_n(t) = \sum_{k=0}^{N-1} F_{n,k} \hat{x}_k(t) - \mu_n^p(t) \hat{s}_n(t-1), \forall n \quad (5)$$

$$\hat{z}_n(t) = \frac{1}{C} \int_{-\infty}^{\infty} z e^{-\frac{(y_n - f(z))^2}{2\alpha\mu^w} - \frac{(\hat{p}_n(t) - z)^2}{2\mu_n^p(t)}} dz, \forall n \quad (6)$$

$$\mu_n^z(t) = \frac{1}{C} \int_{-\infty}^{\infty} z^2 e^{-\frac{(y_n - f(z))^2}{2\alpha\mu^w} - \frac{(\hat{p}_n(t) - z)^2}{2\mu_n^p(t)}} dz - (\hat{z}_n(t))^2, \forall n \quad (7)$$

where

$$C = \int_{-\infty}^{\infty} e^{-\frac{(y_n - f(z))^2}{2\alpha\mu^w} - \frac{(\hat{p}_n(t) - z)^2}{2\mu_n^p(t)}} dz, \forall n \quad (8)$$

$$\hat{s}_n(t) = (1 - \beta) \hat{s}_n(t-1) + \beta \frac{\hat{z}_n(t) - \hat{p}_n(t)}{\mu_n^p(t)}, \forall n \quad (9)$$

$$\mu_n^s(t) = (1 - \beta) \mu_n^s(t-1) + \beta \frac{1 - \frac{\mu_n^z(t)}{\mu_n^p(t)}}{\mu_n^p(t)}, \forall n \quad (10)$$

Step 3) Estimation of input nodes:

$$\tilde{x}_k(t) = (1 - \beta) \tilde{x}_k(t-1) - \beta \hat{x}_k(t) \quad (11)$$

$$\mu_k^r(t) = \left(\frac{1}{N} \sum_{n=0}^{N-1} \mu_n^s(t) \right)^{-1}, \forall k \quad (12)$$

$$\hat{r}_k(t) = \tilde{x}_k(t) + \mu_k^r(t) \sum_{n=0}^{N-1} F_{n,k}^* \hat{s}_n(t), \forall k \quad (13)$$

$$\hat{x}_k(t+1) = \sum_{m=1}^M d_m P_{m,k}, \forall k \quad (14)$$

$$\mu_k^x(t+1) = \sum_{m=1}^M (d_m - \hat{x}_k(t+1))^2 P_{m,k}, \forall k \quad (15)$$

where

$$P_{m,k} = \frac{e^{-\frac{(d_m - \hat{r}_k(t))^2}{2\mu_k^*(t)}}}{\sum_{l=1}^M e^{-\frac{(d_l - \hat{r}_k(t))^2}{2\mu_k^*(t)}}}, \quad (16)$$

M is the number of points in the signal constellation, and $\{d_m\}$ is the vector of constellation points. For example, for 2-PAM modulation, $\{d_m\} = [-1 \quad +1]$, and for 4-PAM modulation $\{d_m\} = [-3/\sqrt{5} \quad -1/\sqrt{5} \quad +1/\sqrt{5} \quad +3/\sqrt{5}]$.

Steps (4)–(15) are repeated with $t \rightarrow t + 1$ until t_{max} iterations have been performed.

We presented here the GAMP algorithm version for the real-valued modulation and real orthogonal transform (e.g. M -PAM and WHT or real-DFT). Nonetheless, the extension to the complex case is straightforward. Moreover, in case of Cartesian-type nonlinearity $f(z)$ the complexity of the decoding algorithm with N complex input symbols is essentially the same as the complexity of the real-valued algorithm with $2N$ input symbols.

More details on the GAMP algorithm and its thorough analysis can be found in [7].

C. Choosing optimal nonlinearity $f(z)$

Choosing the optimal shape of nonlinearity $f(z)$ is not easy, requiring a balance between two conflicting requirements. Firstly, the nonlinear function should be reasonably "chaotic" to guarantee sensitivity to initial conditions and, therefore, random-like properties of the coded waveforms. On the other hand, our experimental study implies that a "truly chaotic" shape of nonlinearity $f(z)$ precludes GAMP algorithm from converging to the ML-solution. Therefore, we adopted an *ad hoc* procedure to select and optimize the shape of the memoryless nonlinearity $f(z)$. Our choice of nonlinearity $f(z)$ relies on two key ideas:

- $f(z)$ should contain a linear or almost linear region around $f(0)$ to allow the message passing decoder to converge.
- $f(z)$ should *resemble* a chaotic iterated function in other regions to guarantee sensitivity to initial conditions.

For a general representation of $f(z)$, we suggest using the flexible, piece-wise linear model:

$$f(z) = \begin{cases} \text{sgn}(z) (a_0 |z| + b_0), & \text{if } 0 \leq |z| < T_1 \\ \text{sgn}(z) (a_1 |z| + b_1), & \text{if } T_1 \leq |z| < T_2 \\ \dots \\ \text{sgn}(z) (a_{i-1} |z| + b_{i-1}), & \text{if } T_{i-1} \leq |z| < T_i \\ \text{sgn}(z) (a_i |z| + b_i), & \text{if } |z| \geq T_i \end{cases} \quad (17)$$

with some parameters $\mathbf{a} = G_0 \{a_0, a_1, \dots, a_i\}$, $\mathbf{b} = \{b_0, b_1, \dots, b_i\}$, and $\mathbf{T} = G_0^{-1} \{0, T_1, T_2, \dots, T_i\}$, where G_0 is a scaling factor that does not affect the "shape" of nonlinearity $f(z)$. For complex modulation (i.e. complex DFT), we apply function (17) separately to the real and imaginary components of z (Cartesian-type nonlinearity). To select the parameters of (17), we devised dozens of different functions $f(z)$ that satisfy the above mentioned heuristic requirements, and then optimized parameter G_0 at our target BER and FER

(namely, $\text{BER} \leq 10^{-5}$, $\text{FER} \leq 1\%$). This non-exhaustive search procedure yielded several "good" sets of parameters \mathbf{a} , \mathbf{b} , and \mathbf{T} , some of which are summarized in Table 1 and illustrated in Figure 2.

TABLE I
EXAMPLE PARAMETERS OF NONLINEARITY $f(z)$

No.	Parameters
1	$\mathbf{a}G_0^{-1} = \{1 \ 2 \ 2 \ -2 \ -2 \ 2 \ 2 \ -2 \ -0.5\}$ $\mathbf{b} = \{0 \ -2 \ -2.5 \ 4 \ 4.5 \ -4 \ -4.5 \ 6 \ 6.5 \ 2.5\}$ $\mathbf{T}G_0 = \{0 \ 1 \ 1.25 \ 1.5 \ 1.75 \ 2 \ 2.25 \ 2.5 \ 2.75 \ 3\}$; $G_0 = 0.53$
2	$\mathbf{a}G_0^{-1} = \{1 \ 2 \ 2 \ -2 \ -2 \ 2 \ 2 \ -2 \ -0.5\}$ $\mathbf{b} = \{0 \ -2 \ -3.5 \ 4 \ 3.5 \ -4 \ -4.5 \ 6 \ 6.5 \ 2.5\}$ $\mathbf{T}G_0 = \{0 \ 1 \ 1.25 \ 1.5 \ 1.75 \ 2 \ 2.25 \ 2.5 \ 2.75 \ 3\}$; $G_0 = 0.5125$
3	$\mathbf{a}G_0^{-1} = \{1.25 \ 2 \ 2 \ -2 \ -2 \ 2 \ 2 \ -2 \ -0.5\}$ $\mathbf{b} = \{0 \ -1.6 \ -3.1 \ 3.6 \ 3.1 \ -3.6 \ -4.1 \ 5.6 \ 6.1 \ 2.4\}$ $\mathbf{T}G_0 = \{0 \ 0.8 \ 1.05 \ 1.3 \ 1.55 \ 1.8 \ 2.05 \ 2.3 \ 2.55 \ 2.8\}$; $G_0 = 0.415$

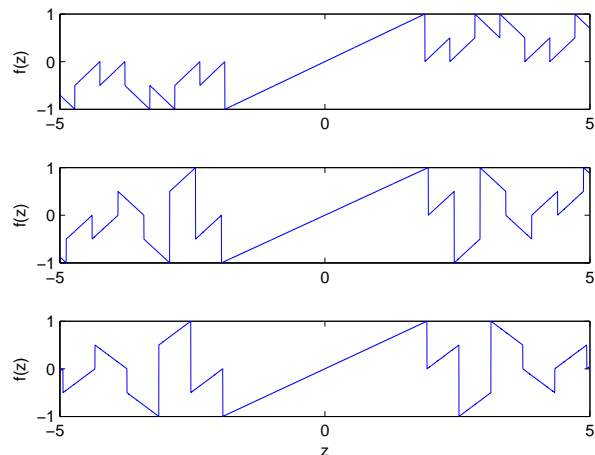


Fig. 2. Three examples of nonlinear functions $f(z)$: nonlinearity 1 (top), nonlinearity 2 (middle), and nonlinearity 3 (bottom).

III. SIMULATION RESULTS

The performance of the proposed modulation scheme with the GAMP-based decoder was studied by means of Monte-Carlo simulation. Our initial simulation-based study revealed that the conventional GAMP algorithm (with $\alpha = 1$, and $\beta = 1$) exhibits several deficiencies, in particular, relatively high error-floor, slow convergence and occasional instability problems (divergence with the increase of number of iterations). It turns out that the error-floor issue was, at least, in part due to the decoder algorithm. To alleviate these deficiencies we implemented several enhancement techniques. Firstly, we appended the cyclic-redundancy check (CRC) block to each data frame and used it for the early stopping criterion. Secondly, after each decoding iteration we calculated the Euclidean distance $E(t)$ between the received vector $\{y_n\}$ and the reconstructed waveform $f\left(\sum_{k=0}^{N-1} F_{n,k} \hat{x}_k(t)\right)$, and if a CRC error was detected after t_{max} iterations the final decision was based on the vector $\{\hat{x}_k(t)\}$ that corresponded to the minimum Euclidean distance $E(t)$. Although this procedure

did not improve FER, it minimized the BER for incorrectly decoded frames. Thirdly, we experimentally discovered that the decoder convergence speed can be significantly improved by using noise scaling factor $\alpha < 1$ simultaneously with damping ($\beta < 1$). However, such a technique could result in occasional algorithm divergence, therefore to achieve better performance we implemented the following procedure: $t_{max}/2$ iterations were performed using the modified GAMP algorithm ($\alpha < 1, \beta < 1$), and if the decoder could not converge within the first $t_{max}/2$ iterations, all internal variables were reset and the subsequent $t_{max}/2$ iterations were performed with the conventional GAMP settings ($\alpha = 1, \beta = 1$). The overall decoding algorithm flowchart is depicted in Figure 3.

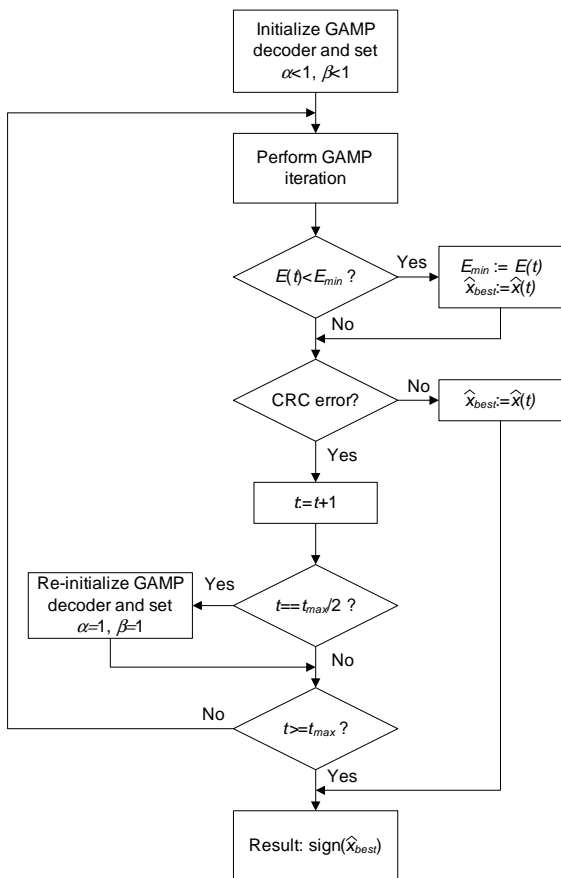


Fig. 3. Decoding algorithm flowchart

Our simulation results indicate that the performance of the proposed scheme with WHT, real DFT or complex DFT with Cartesian-type nonlinearity is almost identical. Therefore, from complexity point of view it seems preferable to use WHT, and, hence, most of our simulation results reported here were obtained for WHT-based scheme.

Figure 4 illustrates the BER vs E_b/N_0 curves for 2-PAM input modulation with three nonlinearities (Table I/Figure 2) and different values of N . In all simulations, the variance of $\{z_n\}$ was normalized to 1, the maximum number of iterations (t_{max}) was set to 100, and integrals (6)–(8) were approximated using numerical summation. At the initialization step the parameters α, β were set to $\alpha = 0.71, \beta = 0.875$.

Remarkably, for the selected nonlinearity parameters $G_0, \mathbf{a}, \mathbf{b}, \mathbf{T}$ the proposed modulation scheme exhibits behavior similar to random-like codes with the presence of a waterfall region and error-floor, and, as expected, performance improves for larger frame sizes. Moreover, the proposed modulation scheme with nonlinearity 3 and $N=16384$ achieves target BER= 10^{-5} at $E_b/N_0 = 3.3$ dB, which represents 6.3 dB gain over uncoded 2-PAM or 4-QAM modulation and is only about 1.5 dB away from the *unconstrained* AWGN channel capacity. These results are better or within $0.1 \div 0.3$ dB of the performance of the capacity-approaching, bandwidth-efficient modulation schemes with $\eta = 2$ bit/s/Hz reported in [1-3, 9, 10]. BER curves for some of these advanced coded modulation schemes with comparable frame sizes are reproduced in Figure 5 for comparison.

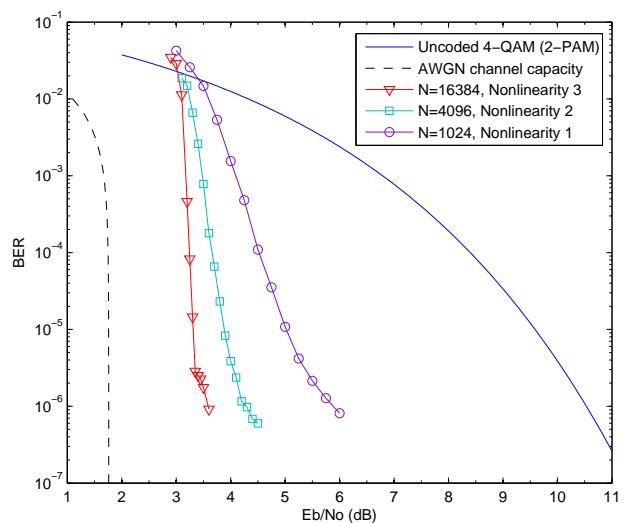


Fig. 4. BER vs E_b/N_0 for the proposed modulation scheme with different nonlinearities and frame sizes in AWGN channel ($\eta = 2$ bit/s/Hz)

Although we set $t_{max} = 100$, the average number of decoder iterations was significantly lower. For example, at $BER = 10^{-5}$ the average number of decoder iterations was about 26 for the frame size $N=16384$, and about 17 for the frame size $N=4096$, and only 7 iterations for the frame size $N=1024$.

A considerable performance improvement over uncoded modulation was also observed for 4-PAM or 16-QAM input modulation ($\eta = 4$ bit/s/Hz). However, in case of 4-PAM/16-QAM, the GAMP algorithm is sub-optimal in terms of BER performance, and the example nonlinearities that we use for 4-QAM/2-PAM (Table I) are not optimal either. Therefore, application of the proposed technique to high-order modulation formats ($\eta \geq 4$ bit/s/Hz) is an open research topic.

IV. DISCUSSION

We believe that the proposed joint coding-modulation technique might be useful in some wired and wireless communication applications, since it has several interesting properties:

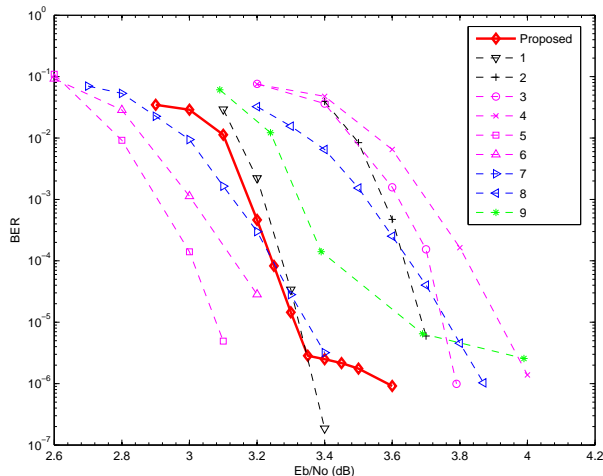


Fig. 5. Performance comparison of the proposed technique (WHT, Nonlinearity 3, $N=16384$) with state-of-the-art coded modulation schemes (2 bit/s/Hz):

- 1) ARJ4A LDPC, $N=16384$, 16-APSK [9],
- 2) ARJ4A LDPC, $N=16384$, 8-PSK [9],
- 3) Regular LDPC, BICM, $d_v=3$, $n=20000$, 4-PAM [1]
- 4) Regular LDPC, BICM, $d_v=3$, $n=10000$, 4-PAM [1]
- 5) Irregular LDPC, BICM, $d_v=15$, $n=20000$, 4-PAM [1]
- 6) Irregular LDPC, BICM, $d_v=15$, $n=10000$, 4-PAM [1]
- 7) eIRA LDPC, BICM, $n=10000$, 4-PAM [10]
- 8) eIRA LDPC, BICM, $n=9000$, 8-PSK [10]
- 9) Turbo TCM, $N=10000$, 8-PSK [3]

- Good BER performance: As illustrated in the previous section the BER performance is on par with that of the best known coded modulation schemes.
- Relatively low decoder complexity: The GAMP-based decoder complexity per iteration is dominated by two orthogonal transform operations, which, in case of fast WHT, require only $N \log_2(N)$ real additions or subtractions. The input/output nonlinear step is generally a scalar operation with complexity of order $O(N)$. Although, in our simulation model, we used numerical integration to approximate integrals (6)–(8), these can be expressed in closed-form using tabulated Gauss error function, and, consequently, can be simplified or implemented via lookup tables. It is also possible to use simpler max-sum version of the GAMP algorithm to trade-off performance and complexity [7].
- The choice of nonlinearity $f(z)$ may be tailored to the requirements of the transmission system in order to improve overall system efficiency. For example, $f(z)$ may be selected to improve power conversion efficiency, or illumination-to-communication conversion efficiency in visible light communication applications [11].
- An interesting application of the proposed modulation scheme is to use it in combination with a conventional, linear OFDM transmitter, as illustrated in Figure 6. Such a system arrangement may result in the OFDM signal with reduced PAPR. Due to the presence of nonlinearity $f(z)$, the distribution of signal samples at the output of the modulator illustrated in Figure 6 resembles the distribution of M -QAM/ M -PAM signal affected by additive

Gaussian noise. It can be shown that if the nonlinearity $f(z)$ has a relatively large linear region the PAPR of such a signal will be much lower than that of a conventional OFDM signal. Figure 7 compares the complementary cumulative distribution functions (CCDF) of PAPR for signals generated by the transmission system illustrated in Figure 6 with nonlinearity 1 (complex-valued OFDM with Cartesian-type nonlinearity), and a conventional OFDM system. We analyzed CCDF for Nyquist sampled waveforms and four-times oversampled waveforms, since four-times oversampling provides a good approximation of the continuous-time PAPR [12]. As may be seen, at probability 10^{-4} the PAPR of the continuous signal generated by the transmission system illustrated in Figure 6 is approximately 2.3 dB lower than the PAPR of a conventional OFDM signal. The difference is increased to 3.9dB for Nyquist-sampled waveforms.

It should be noted that the proposed method has several limitations and open issues. Firstly, in this paper, we focused primarily on the case $\eta = 2$ bit/s/Hz. One possible way to apply this technique to systems with higher spectral efficiency is to use the output waveform puncturing. This approach (i.e. random puncturing) seems to work well up to $\eta = 2.5 \div 3$ bit/s/Hz. It is also possible to use higher-order input modulations (16-QAM/4-PAM), however, as we mentioned earlier, extension of this technique to spectral efficiency $\eta \geq 4$ bit/s/Hz is still an open research topic. Secondly, the GAMP algorithm is based on Gaussian and quadratic approximations, and, therefore, it is apparently sub-optimal, especially, for small frame sizes. We were able to improve performance of the GAMP-based decoder using several *ad hoc* techniques. However, it is still unclear, how close the GAMP decoder performance is to the theoretical ML performance. Finally, our choice of nonlinearity $f(z)$ is generally based on a heuristic and experimental approach. The problem here is that the performance of the proposed scheme is limited not only by distance distribution of encoded waveforms but also by non-idealities of the decoding algorithm, and this fact greatly complicates optimization strategy.

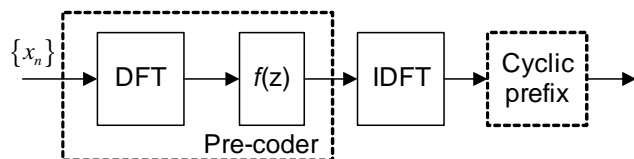


Fig. 6. Proposed modulation scheme as a pre-coder for a conventional OFDM transmitter

V. CONCLUSIONS

In this paper, we proposed a novel joint coding-modulation technique based on serial concatenation of orthogonal linear transformation (e.g., WHT or DFT) with memoryless nonlinearity. We demonstrated that such a simple signal construction may exhibit properties of a random code ensemble, as a result approaching channel capacity. Our computer simulations confirmed that if the decoder relies on the approximate message

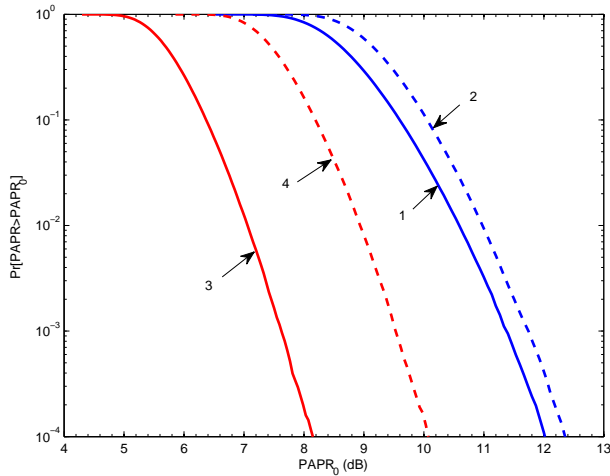


Fig. 7. CCDF of PAPR for the proposed pre-coded OFDM (Figure 6) with $N=1024$ and nonlinearity #1:

- 1) Conventional OFDM (Nyquist sampling)
- 2) Conventional OFDM (four-times oversampling)
- 3) OFDM with the proposed modulation (Nyquist sampling)
- 4) OFDM with the proposed modulation (four-times oversampling)

passing algorithm, the proposed modulation technique exhibits performance on par with state-of-the-art coded modulation schemes that use capacity-approaching component codes. The proposed technique could be extended to modulation formats with higher spectral efficiency ($\eta \geq 4$ bit/s/Hz) and other types of orthogonal transformations, offering one possible direction for our future research.

REFERENCES

- [1] J. Hou, *et al.*, "Capacity-approaching bandwidth-efficient coded modulation schemes based on low-density parity-check codes," *IEEE Trans. Inf. Theory*, vol. 49, no. 9, pp. 2141–2155, Sep. 2003.
- [2] D. Divsalar and C. Jones, "Protograph based low error floor LDPC coded modulation," in *Proc. 2005 IEEE Military Communications Conf.*, Atlantic City, NJ, Oct. 2005, pp. 378–385.
- [3] P. Robertson and T. Woz, "Bandwidth-efficient turbo trellis-coded modulation using punctured component codes," *IEEE J. Sel. Areas Commun.*, vol. 16, no. 2, pp. 206–218, Feb. 1998.
- [4] J. Guerreiro, R. Dinis and P. Montezuma, "On the optimum multicarrier performance with memoryless nonlinearities," *IEEE Trans. Commun.*, vol. 63, no. 2, pp. 498–509, Feb. 2015.
- [5] S. Zhidkov, "Detection of nonlinearly distorted OFDM signals via generalized approximate message passing," arXiv:1703.01562 [cs.IT], Mar 2017.
- [6] J. C. Sprott, *Chaos and Time-Series Analysis*. Oxford University Press, 2003.
- [7] S. Rangan, "Generalized approximate message passing for estimation with random linear mixing," in *Proc. IEEE Int. Symp. Information Theory*, Saint-Petersburg, Russia, 2011, pp. 2174–2178. (extended version available at arXiv:1010.5141 [cs.IT]).
- [8] S. Rangan, P. Schniter, and A. Fletcher, "On the convergence of generalized approximate message passing with arbitrary matrices," in *Proc. IEEE Int. Symp. Information Theory*, July 2014, pp. 236–240, (extended version available at arXiv:1402.3210 [cs.IT]).
- [9] J. Hamkins, "Performance of low-density parity-check coded modulation," in *Proc. 2010 IEEE Aerospace Conference*, Big Sky, MT, 2010, pp. 1–14.
- [10] G. Durisi, L. Dinioi, and S. Benedetto, "eIRA codes for coded modulation systems," in *Proc. IEEE Int. Conf. on Comm.*, Istanbul, Turkey, Jun. 2006, vol. 3, pp. 1125–1130.
- [11] Z. Yu, R. J. Baxley and G. T. Zhou, "Peak-to-average power ratio and illumination-to-communication efficiency considerations in visible light OFDM systems," in *Proc. IEEE Int. Conf. on Acoustics, Speech and Signal Processing*, Vancouver, BC, 2013, pp. 5397–5401.
- [12] K. D. Wong, M. O. Pun and H. V. Poor, "The continuous-time peak-to-average power ratio of OFDM signals using complex modulation schemes," *IEEE Trans. on Commun.*, vol. 56, no. 9, pp. 1390–1393, Sep. 2008.